

Electroweak and supersymmetric two-loop corrections to $(g - 2)_\mu$

S. HEINEMEYER^{1*}, D. STÖCKINGER^{2†} AND G. WEIGLEIN^{2‡}

¹ *CERN, TH Division, Dept. of Physics, 1211 Geneva 23, Switzerland*

² *Institute for Particle Physics Phenomenology, University of Durham,
Durham DH1 3LE, UK*

Abstract

We present the up to now most precise evaluation of electroweak and supersymmetric contributions to the anomalous magnetic moment of the muon a_μ , describing in detail also the calculational techniques. We calculate the bosonic two-loop contributions in the Standard Model without the approximation of a heavy Higgs-boson mass, finding corrections up to 0.2×10^{-10} for a light Higgs boson. In the Minimal Supersymmetric Standard Model the corresponding two-loop contributions from the two-Higgs-doublet model part differ from the Standard Model result by up to 0.3×10^{-10} . Finally, we evaluate the diagrams where a loop of charginos or neutralinos, the superpartners of gauge and Higgs bosons, is inserted into a two-Higgs-doublet one-loop diagram. These corrections can amount up to 10×10^{-10} , which is almost 2σ of the current experimental uncertainty.

*email: Sven.Heinemeyer@cern.ch

†email: Dominik.Stockinger@durham.ac.uk

‡email: Georg.Weiglein@durham.ac.uk

1 Introduction

The final result of the Brookhaven “Muon $g-2$ Experiment” (E821) for the anomalous magnetic moment of the muon, $a_\mu \equiv (g-2)_\mu/2$, reads [1]

$$a_\mu^{\text{exp}} = (11\,659\,208 \pm 6) \times 10^{-10} . \quad (1)$$

The Standard Model (SM) prediction depends on the evaluation of the hadronic vacuum polarization and light-by-light contributions. The former have been evaluated by Refs. [2–5], the latter by Ref. [6], but there is a recent reevaluation [7], describing a possible shift of the central value by 5.6×10^{-10} . Depending on which hadronic evaluation is chosen, the difference between experiment and the SM prediction lies between the two values¹

$$a_\mu^{\text{exp}} - a_\mu^{\text{theo}} ([3]+[6]) = (31.7 \pm 9.5) \times 10^{-10} : 3.3 \sigma , \quad (2)$$

$$a_\mu^{\text{exp}} - a_\mu^{\text{theo}} ([2]+[7]) = (20.2 \pm 9.0) \times 10^{-10} : 2.1 \sigma . \quad (3)$$

These evaluations are all e^+e^- data driven. Recent analyses concerning τ data indicate that uncertainties due to isospin breaking effects may have been underestimated earlier [4]. For the purpose of numerical comparisons we will use the intermediate value

$$a_\mu^{\text{exp}} - a_\mu^{\text{theo}} ([3]+[7]) = (24.5 \pm 9.0) \times 10^{-10} : 2.7 \sigma . \quad (4)$$

It is an interesting question whether the observed $2-3\sigma$ deviation is due to supersymmetric effects. The supersymmetric one-loop contribution [9] is approximately given by

$$a_\mu^{\text{SUSY,1L}} = 13 \times 10^{-10} \left(\frac{100 \text{ GeV}}{M_{\text{SUSY}}} \right)^2 \tan \beta \text{sign}(\mu), \quad (5)$$

if all supersymmetric particles (the relevant ones are the smuon, sneutralino, chargino and neutralino) have a common mass M_{SUSY} . Obviously, supersymmetric effects can easily account for a $(20 \dots 30) \times 10^{-10}$ deviation, if μ is positive and M_{SUSY} lies roughly between 100 GeV (for small $\tan \beta$) and 600 GeV (for large $\tan \beta$). This mass range is both allowed by present search limits and very interesting in view of physics at Run II of the Tevatron, the LHC and a future Linear Collider (LC).

Eq. (5) also shows that for certain parameter choices the supersymmetric contributions could have values of either $a_\mu^{\text{SUSY}} \gtrsim 60 \times 10^{-10}$ or $a_\mu^{\text{SUSY}} \lesssim -10 \times 10^{-10}$, both outside the 3σ band of the allowed range according to (2), (3). This means that the $(g-2)_\mu$ measurement places strong bounds on the supersymmetric parameter space. This is important for constraining different variants of supersymmetric models (and of course also other models of new physics) and complements the direct searches. Even after the discovery of supersymmetric particles, indirect bounds derived from $(g-2)_\mu$

¹We always include the updated QED result from Ref. [8].

or b -decays and a Higgs mass measurement will provide important complementary information to that obtained from direct measurements.

In order to fully exploit the precision of the $(g-2)_\mu$ experiment within Supersymmetry (SUSY), see Refs. [10,11] for possible applications, the theoretical uncertainty of the SUSY loop contributions from unknown higher-order corrections should be significantly lower than the experimental error given in eq. (1) and the hadronic uncertainties in the SM prediction. Thus, the reduction of the uncertainty of the SUSY loop contributions down to the level of about $\pm 1 \times 10^{-10}$ is desirable.

For the electroweak part of the SM prediction this accuracy has been reached with the computation of the complete two-loop result [12,13]. However, this result relies on a single evaluation of the bosonic two-loop contributions, performed in the limit of a heavy SM Higgs-boson mass, $M_{HSM} \gg M_W$. Thus, an independent check seems desirable. In this paper we perform this evaluation for arbitrary Higgs-boson masses.

For the SUSY contributions, a similar level of accuracy has not been reached yet, since the corresponding two-loop corrections are largely unknown. Only two parts of the two-loop contribution have been evaluated up to now. The first part are the leading $\log(m_\mu/M_{SUSY})$ -terms of supersymmetric one-loop diagrams with a photon in the second loop. They amount to about -8% of the supersymmetric one-loop contribution (for a SUSY mass scale of $M_{SUSY} = 500$ GeV) [14].

The second known part are the diagrams with a closed loop of SM fermions or scalar fermions calculated in Ref. [15], extending previous results of Refs. [16,17]. It has been shown in Ref. [15] that the numerical effect of these contributions could in principle be as large as 20×10^{-10} for suitable parameter choices. But experimental constraints on the lightest Higgs-boson mass [18–21], electroweak precision observables [22–24] and b -decays [25,26] restrict the allowed parameter space. Thus the values of these diagrams amount up to about 5×10^{-10} , except in rather restricted parameter regions with non-universal sfermion mass parameters involving very disparate mass scales.

In general, every diagram in the Minimal Supersymmetric Standard Model (MSSM) must contain one continuous line carrying the μ -lepton number. Thus, the MSSM diagrams can be divided into two classes: (1) diagrams containing a one-loop diagram involving supersymmetric particles (with a $\tilde{\mu}$ or $\tilde{\nu}_\mu$ line) to which a second loop is attached, and (2) diagrams where a second loop is attached to a two-Higgs-doublet model one-loop diagram (with a μ or ν_μ line). The QED-logarithms from Ref. [14] belong to the first class, and the fermion/sfermion two-loop diagrams from Ref. [15] to the second.

The diagrams of the second class are particularly interesting since they can depend on other parameters than the supersymmetric one-loop diagrams and can therefore change the qualitative behaviour of the supersymmetric contribution to a_μ . In particular, they could even be large if the one-loop contribution is suppressed, e.g. due to heavy smuons and sneutrinos.

In this paper we complete the calculation of the diagrams of this class. As the first step we calculate all pure two-Higgs-doublet model diagrams. This calculation is analogous to the one of the SM bosonic two-loop corrections (we carry out the calculation of the SM contributions as a special case), but it involves the additional Higgs bosons (but no SUSY particles). The second step comprises the diagrams with a closed chargino/neutralino loop. Their structure is similar to the one of diagrams with a closed SM fermion or sfermion loop, but they depend on a completely different set of parameters and show a complementary behavior.

The objective of this paper is to describe in detail the calculational steps, which have already been used in Ref. [15], and to analyze the numerical impact of the newly derived SUSY contributions. The SM result is compared to the existing calculation. As for the results of Ref. [15], the new results will be implemented into the Fortran code *FeynHiggs* [27].

The outline is as follows. In Sect. 2 we describe the calculation, in particular the used regularization, large mass expansion, reduction of two-loop integrals, and renormalization. For the two-loop QED corrections involving SUSY particles analytical results are presented. Section 3 is devoted to the SM contributions. The numerical results for the two-Higgs-doublet contribution in the MSSM and the chargino/neutralino contribution are discussed in Sects. 4 and 5, respectively. Our conclusions are given in Sect. 6.

2 Calculation

2.1 Extraction of a_μ

The anomalous magnetic moment a_μ of the muon is related to the photon–muon vertex function $\Gamma_{\mu\bar{\mu}A\rho}$ as follows:

$$\begin{aligned}\bar{u}(p')\Gamma_{\mu\bar{\mu}A\rho}(p, -p', q)u(p) &= \bar{u}(p') [\gamma_\rho F_V(q^2) + (p + p')_\rho F_M(q^2) + \dots] u(p), \\ a_\mu &= -2m_\mu F_M(0).\end{aligned}\tag{6}$$

It can be extracted from the regularized vertex function using the projector [12, 13]

$$\begin{aligned}a_\mu &= \frac{1}{2(D-1)(D-2)m_\mu^2} \text{Tr} \left\{ \frac{D-2}{2} [m_\mu^2 \gamma_\rho - D p_\rho \not{p} - (D-1)m_\mu p_\rho] V^\rho \right. \\ &\quad \left. + \frac{m_\mu}{4} (\not{p} + m_\mu) (\gamma_\nu \gamma_\rho - \gamma_\rho \gamma_\nu) (\not{p} + m_\mu) T^{\rho\nu} \right\},\end{aligned}\tag{8}$$

$$V_\rho = \Gamma_{\mu\bar{\mu}A\rho}(p, -p, 0),\tag{9}$$

$$T_{\rho\nu} = \left. \frac{\partial}{\partial q^\rho} \Gamma_{\mu\bar{\mu}A\nu}(p - (q/2), -p - (q/2), q) \right|_{q=0}.\tag{10}$$

Here the muon momentum is on-shell, $p^2 = m_\mu^2$, and D is the dimension of space-time.

This projector requires that in the covariant decomposition (6) only D -dimensional quantities appear. We therefore use dimensional regularization with anti-commuting γ_5 , where there is no distinction between the first four and the remaining $D - 4$ dimensions. However, in order to demonstrate the validity of this regularization we need to discuss three issues related to supersymmetry breaking, mathematical consistency and the treatment of the ϵ -tensor in this scheme.

- Dimensional regularization breaks supersymmetry [28], and in general supersymmetry has to be restored by adding certain counterterms not corresponding to multiplicative renormalization of the fields and parameters [29]. In our case, however, all appearing counterterms are two-Higgs-doublet model counterterms, because we calculate 2-loop corrections to 1-loop two-Higgs-doublet model diagrams, see also Sect. 2.3. These two-Higgs-doublet model counterterms are either fixed by renormalization conditions, like the muon- or Z -mass counterterm, or by gauge invariance, like the $\mu\mu\gamma$ - or $W^+G^-\gamma$ -counterterms. Since gauge invariance is not broken by dimensional regularization with anti-commuting γ_5 ,² multiplicative renormalization is sufficient for all counterterms in our calculation.
- Using an anti-commuting γ_5 in $D \neq 4$ implies $\text{Tr}(\gamma_5\gamma^\mu\gamma^\nu\gamma^\rho\gamma^\sigma) = 0$ and is therefore incompatible with the trace formula $\text{Tr}(\gamma_5\gamma^\mu\gamma^\nu\gamma^\rho\gamma^\sigma) \propto \epsilon^{\mu\nu\rho\sigma}$, which has to be reproduced for $D \rightarrow 4$. As it is customary, we simply replace each trace of the form $\text{Tr}(\gamma_5\gamma^\mu\gamma^\nu\gamma^\rho\gamma^\sigma)$ by its four-dimensional value. We can check the correctness of this procedure by comparing the terms involving ϵ -tensors with the ones obtained using the HVBM-scheme [31], which is fully consistent. In our calculation, ϵ -tensors appear only in two-loop diagrams with an insertion of a fermion triangle with three external vector bosons. The difference of the fermion triangle subdiagrams in the two schemes (summed over one generation or all charginos and neutralinos) is of the order $(D - 4)\frac{k_\sigma}{k^2} \epsilon^{\mu\nu\rho\sigma}$, where k_σ is the non-vanishing external momentum of the fermion triangles. The covariant $\epsilon^{\mu\nu\rho\sigma} k_\sigma$ of power-counting degree +1 has the same prefactor as the chiral gauge anomaly and thus vanishes. If the fermion triangles are inserted into 1-loop diagrams contributing to $\Gamma_{\mu\bar{\mu}A\rho}$, the difference between the naive and the HVBM-scheme vanishes for $D \rightarrow 4$ for power-counting reasons. Hence, the terms involving ϵ -tensors are identical in the naive and the HVBM-scheme, which means that the naive scheme produces these terms correctly (see also the discussion in Ref. [30]).
- The ϵ -tensor is a purely four-dimensional object, and contractions like $\epsilon^{\mu\alpha\beta\gamma}\epsilon^\nu_{\alpha\beta\gamma}$ or $\epsilon^{\mu\nu\alpha\beta}\epsilon^{\rho\sigma}_{\alpha\beta}$ have to be evaluated in four dimensions.³ Effectively, this leads to the appearance of the additional covariant $\gamma_\rho^{4-\text{dim}}F_V^{4-\text{dim}}$ in eq. (6). This contradicts the requirement of the projection (8) that only D -dimensional covari-

²This has been checked up to the order we need here in Ref. [30].

³We checked explicitly that a D -dimensional treatment indeed leads to incorrect results.

ants may appear in $\Gamma_{\mu\bar{\mu}A\rho}$. However, as mentioned above, the fermion triangle subdiagrams add up to an expression of reduced power-counting degree, and accordingly the ϵ -tensor contributions to $\Gamma_{\mu\bar{\mu}A\rho}$ and thus $F_V^{4-\text{dim}}$ are finite. As a result, the projection operator (8) produces the correct result, containing only the form factor F_M , even if the ϵ -tensors are evaluated in four dimensions.

2.2 Diagram evaluation

The actual calculation is done using computer algebra. The Feynman diagrams are generated using *FeynArts* [32,33]. After applying the projector (8), the Dirac algebra, traces and contractions are performed by *TwoCalc* [34].

The main part of the two-loop calculation consists of the evaluation of the two-loop integrals and the simplification of their coefficients, both of which is complicated by the large number of different mass scales and the involved structure of the MSSM Feynman rules.

As a first step we perform a large mass expansion [35] in the ratio m_μ/M_{heavy} , where M_{heavy} stands for all heavy masses, $M_{Z,W}$ and Higgs and chargino/neutralino masses. Depending on the prefactors we expand all integrals to sufficiently high order such that the final result is correct up to $\mathcal{O}(m_\mu^2/M_{\text{heavy}}^2)$. We discard all terms of $\mathcal{O}(m_\mu^4/M_{\text{heavy}}^4)$. The expansion is based on the formula [35]

$$F_\Gamma \sim \sum_\gamma F_{\Gamma/\gamma} \circ \mathcal{T}_\gamma F_\gamma. \quad (11)$$

Here F_Γ denotes the integral corresponding to a (two-loop) Feynman diagram Γ , Γ/γ denotes the diagram where the subdiagram γ is shrunk to a point and \mathcal{T}_γ denotes Taylor expansion with respect to all small masses and all external momenta of γ . The sum runs over all (in general unconnected) subdiagrams γ that

- contain all lines with heavy masses,
- are one-particle irreducible with respect to the light lines.

By means of (11) the large masses appear only in γ , whereas the small masses and momenta appear only in Γ/γ , resulting in a separation of scales. Since the projection operator (8) sets the external photon momentum to zero, our integrals are initially two-loop two-point integrals. There are therefore three possibilities for the r.h.s. of the large mass expansion (11) and the subsequent reduction to master integrals:

- (Light 0-loop) \circ (heavy 2-loop): In this case, the r.h.s. of (11) results in a two-loop vacuum diagram times a rational function of m_μ . Using partial integration identities [36], we reduce all two-loop vacuum diagrams to the master integral

$$T_{134}(m_1, m_3, m_4) = \left\langle \left\langle \frac{1}{D_1 D_3 D_4} \right\rangle \right\rangle \quad (12)$$

in the notation of [34]:

$$D_i = k_i^2 - m_i^2, \quad (13)$$

$$k_1 = q_1, \quad k_2 = q_1 + p, \quad k_3 = q_2 - q_1, \quad (14)$$

$$k_4 = q_2, \quad k_5 = q_2 + p, \quad (15)$$

$$\langle\langle \dots \rangle\rangle = \int \frac{d^D q_1 d^D q_2}{[i\pi^2(2\pi\mu)^{D-4}]^2}(\dots). \quad (16)$$

The result for the general case of three different masses can be found e.g. in Ref. [37].

- (Light 1-loop) \circ (heavy 1-loop): In this case the integrals can be reduced to the standard one-loop functions $A_0(m)$ and $B_0(m_\mu^2, 0, m_\mu)$ [38].
- (Light 2-loop) \circ (heavy 0-loop): This case appears e.g. in the calculation of diagrams 7,8 in Fig. 3 below. In general it can only appear in diagrams that do not involve any SUSY particles, since SUSY particles (in scenarios with R-parity conservation) necessarily form at least one closed heavy loop. The r.h.s. of (11) then contains two-loop two-point functions, however with only one mass scale, m_μ . One typical example of such integrals is

$$Y_{2334}^{1155}(m_\mu^2; m_\mu, m_\mu, m_\mu) = \langle\langle \frac{(k_1^2)^2 (k_5^2)^2}{D_2 D_3^2 D_4} \rangle\rangle. \quad (17)$$

with $p^2 = m_\mu^2$ and $m_{2,3,4} = m_\mu$. Using Passarino-Veltman decomposition for the one-loop subdiagrams [34] and partial integration identities all such integrals can be reduced to one-loop integrals and the on-shell (i.e. $p^2 = m_\mu^2$) master two-loop sunset integrals $T_{234}(m_\mu^2; m_\mu, m_\mu, m_\mu)$ and $T_{234}(m_\mu^2; m_\mu, 0, 0)$. For example, for (17) we obtain

$$\begin{aligned} Y_{2334}^{1155}(m_\mu^2; m_\mu, m_\mu, m_\mu) = & \\ & \frac{4(-4 + 19D - 31D^2 + 14D^3)}{8 - 18D + 9D^2} m_\mu^4 A_0(m_\mu)^2 \\ & + \frac{32(-2 + D)D^2}{3(8 - 18D + 9D^2)} m_\mu^6 T_{234}(m_\mu^2; m_\mu, m_\mu, m_\mu). \end{aligned} \quad (18)$$

For the analytical results of on-shell two-loop two-point functions, see Ref. [39] and references therein. Note that the reduction can generate spurious additional divergences, in the form of $1/(D-4)$ -poles in prefactors of master integrals. A simple example is given by the reduction of Y_{2345}^1 with $p^2 = m_\mu^2$ and $m_{2,3,4} = m_\mu$, $m_5 = 0$:

$$\begin{aligned} Y_{2345}^1(m_\mu^2; m_\mu, m_\mu, m_\mu, 0) = & \\ & -\frac{1}{2(D-4)} \left\{ 4A_0(m_\mu) B_0(m_\mu^2, 0, m_\mu) \right. \\ & \left. + (D-2) \left[\frac{A_0(m_\mu)^2}{m_\mu^2(D-3)} - 2T_{234}(m_\mu^2; m_\mu, m_\mu, m_\mu) \right] \right\}. \end{aligned} \quad (19)$$

Although the $1/(D-4)^3$ -poles cancel, the analytical results of the master integrals are needed up to $\mathcal{O}(D-4)$ in the case of T_{234} and up to $\mathcal{O}((D-4)^2)$ in the case of A_0 and B_0 functions.

2.3 Counterterm contributions

Since a_μ is exactly zero at tree-level, no two-loop counterterm corrections arise. However, one-loop diagrams with counterterm insertion are necessary to derive a UV-finite result. Thus, together with the two-loop diagrams we have also evaluated all the diagrams with subloop renormalization in the SM and the MSSM.

In order to derive the amplitudes of the diagrams with counterterm insertion it was necessary to extend the existing *FeynArts* MSSM model file [33] by including non-SM counterterm vertices. The introduced counterterms contain field renormalization constants for the gauge and Higgs bosons and for the muon and the neutrino. We have checked that in the sum of all amplitudes all field renormalization constants, except of the external muon and photon, drop out as required. In addition to the field renormalization constants also mass counterterms for the SM gauge bosons and the muon have been introduced. Finally, counterterms for the Higgs sector arising from the Higgs potential (see e.g. Ref. [20]) as well as for the mixing of Higgs- and gauge bosons have been included. The Higgs sector counterterms consist, besides field renormalization constants, of Higgs tadpoles that cancel large corrections coming from the self-energy insertions at the two-loop level.

We have chosen on-shell renormalization conditions for the muon and the photon, for the W - and Z -boson masses, and for the electric charge. The tadpole counterterms cancel their corresponding loop contributions.

Since all amplitudes are reduced to self-energy like corrections, the result of the counterterm diagrams consists only of A_0 and B_0 functions. As for the genuine two-loop diagrams, also for the counterterm diagrams a large mass expansion is necessary in order to obtain a consistent expansion in powers of m_μ .

As already outlined in Ref. [15] we parametrize our one-loop result with G_μ in order to absorb process-independent higher-order corrections. This requires the evaluation of the one-loop corrections to muon decay, Δr , from the corresponding sectors. For the class of corrections evaluated in Ref. [15], all contributions to Δr from scalar fermion diagrams (since the SM fermions contribute only to the SM result) had to be taken into account. For the results computed in the present paper the Δr corrections from charginos and neutralinos, as well as from the whole two-Higgs-doublet sector of the MSSM (except fermions) had to be evaluated. While the former ones consist only of self-energy corrections, the latter ones also contain vertex and box contributions involving SM particles. The Δr contribution enters via $(-a_\mu^{1L} \Delta r)$, where a_μ^{1L} is the two-Higgs-doublet model one-loop result. In the case of the SM gauge and Higgs-boson contributions the Δr term amounts to a shift in the two-loop corrections of about 10%.

2.4 QED contributions

In general, the contributions to a_μ can be split into QED and electroweak contributions. A diagram is counted as a QED diagram if it involves only the photon but no other gauge or Higgs boson, and as an electroweak diagram if it contains a W , Z or Higgs boson (or some of the corresponding ghost fields).

At the two-loop level, there are QED diagrams involving a photon vacuum polarization subdiagram (see Fig. 1). For leptons or quarks, these contributions are of course known; in the latter case they have to be obtained via the hadronic vacuum polarization [2–5].

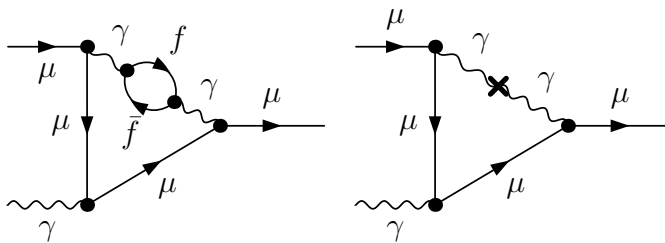


Figure 1: Generic QED diagrams with a fermion loop insertion (left) and the corresponding counterterm diagram (right). The same kind of diagram exists with a scalar inserted instead of a fermion.

If supersymmetric particles contribute, the two-loop QED contributions are modified by the diagrams of Fig. 1 with a chargino, slepton, or squark loop. In our calculations in the following sections, as well as in Ref. [15], we do not include these QED contributions. They can be easily inferred from known results [40] and are tiny. For completeness, we list the results here. The result of these diagrams depends only on the charge Q , the mass M , and the spin of the particle in the vacuum polarization. For a scalar particle we have

$$a_\mu^{\text{QED,2L,scalar}} = \frac{Q^2}{360} \left(\frac{\alpha}{\pi}\right)^2 \frac{m_\mu^2}{M^2}, \quad (20)$$

and for a fermionic particle we have

$$a_\mu^{\text{QED,2L,fermionic}} = \frac{Q^2}{45} \left(\frac{\alpha}{\pi}\right)^2 \frac{m_\mu^2}{M^2}. \quad (21)$$

For masses $M \gtrsim 100$ GeV, these contributions are below 10^{-13} and hence negligible.

The results in (20), (21) contain the suppression factor m_μ^2/M^2 , which is typical for all diagrams except for the pure QED-ones involving only photons and muons. However, this only holds after renormalization, i.e. for the sum of the two-loop diagrams and the counterterm insertions. The two-loop diagram in Fig. 1 itself has a

contribution of the order m_μ^0 , which is then cancelled by the counterterm diagram. The reason is that before renormalization, the vacuum polarization subdiagram including the two photon propagators behaves like $\frac{1}{k^2}\Pi^\gamma(k^2)\frac{1}{k^2} \propto \frac{1}{k^2}$ for $k^2 \rightarrow 0$, like the tree-level photon propagator, whereas after renormalization (here charge and field renormalization effectively amount to adding the counterterm diagram in Fig. 1) we have $\frac{1}{k^2}\hat{\Pi}^\gamma(k^2)\frac{1}{k^2} \propto 1$ for $k^2 \rightarrow 0$.

3 Standard Model contributions

Before discussing the MSSM results, we present our results for the bosonic electroweak two-loop contributions in the SM. Up to now, there exists only one evaluation of these diagrams [12], which employs the approximation $M_{H^{\text{SM}}} \gg M_W$. Our recalculation of these contributions serves both as a cross check of Ref. [12] and of our algebraic codes. It furthermore allows to compare the approximation of Ref. [12] with the result for arbitrary $M_{H^{\text{SM}}}$.

Some typical diagrams of this class are shown in Fig. 3 below, if one identifies ϕ with the SM Higgs boson and ψ with the charged Goldstone boson of the SM (in the Feynman gauge). In general this class consists of all SM two-loop diagrams without a closed fermion loop and without pure QED diagrams. We obtain the following result:

$$a_\mu^{\text{bos},2\text{L}} = \frac{5}{3} \frac{G_\mu m_\mu^2}{8\pi^2 \sqrt{2}} \frac{\alpha}{\pi} \left(c_L^{\text{bos},2\text{L}} \log \frac{m_\mu^2}{M_W^2} + c_0^{\text{bos},2\text{L}} \right), \quad (22)$$

where the coefficient of the large logarithm, $\log \frac{m_\mu^2}{M_W^2} \approx -13$, can be written in analytical form:

$$c_L^{\text{bos},2\text{L}} = \frac{1}{30} [107 + 23(1 - 4s_w^2)^2] \approx 3.6, \quad (23)$$

in agreement with Ref. [12]. The coefficient $c_0^{\text{bos},2\text{L}}$ has a more involved analytical form. In Fig. 2 we show the results for $a_\mu^{\text{bos},2\text{L}}$ from eq. (22) as a function of $M_{H^{\text{SM}}}$. The variation comes from the non-logarithmic piece $c_0^{\text{bos},2\text{L}}$. The size of the (constant) logarithmic contributions is also indicated. It can be seen that the variation with $M_{H^{\text{SM}}}$ is at the level of 0.3×10^{-10} for $100 \text{ GeV} \lesssim M_{H^{\text{SM}}} \lesssim 500 \text{ GeV}$. These numerical values also confirm the results of Ref. [12]. The logarithmic piece in (22) alone is already a very good approximation and leads to

$$a_\mu^{\text{bos},2\text{L}} = (-2.2 \pm 0.2) \times 10^{-10}, \quad (24)$$

corresponding to a reduction of the electroweak one-loop contribution by about 11%.

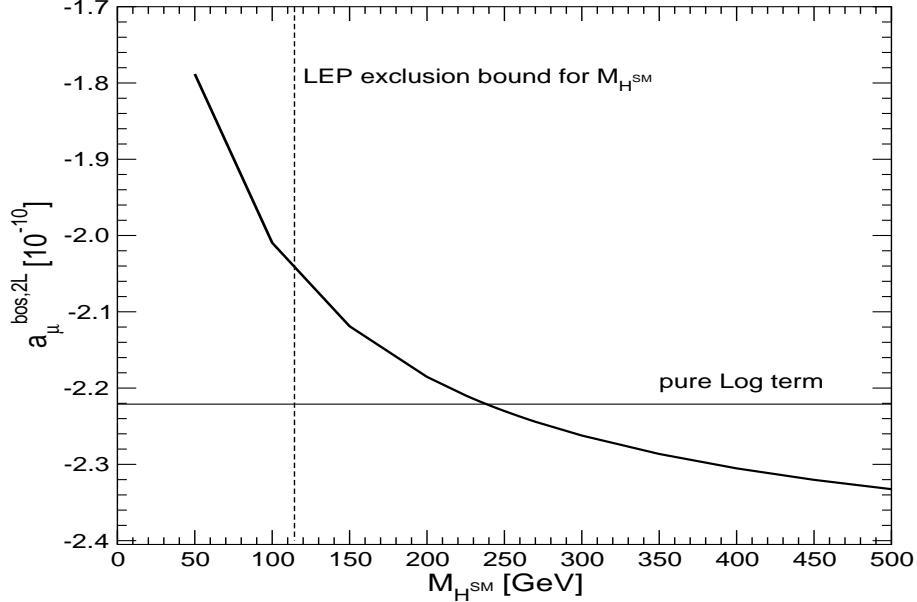


Figure 2: $a_\mu^{\text{bos},2L}$ is shown as a function of $M_{H^{\text{SM}}}$, see eq. (22). The size of the (constant) logarithmic contributions is also indicated.

4 Two-Higgs-doublet contributions

In the MSSM, the bosonic electroweak two-loop contributions are different compared to the SM because of the extended MSSM Higgs sector. In this section we present the result for the contributions of this class, defined by selecting all MSSM two-loop diagrams without a closed loop of fermions or sfermions and without pure QED-diagrams, see Fig. 3.

The result $a_\mu^{\text{bos},2L,\text{MSSM}}$ reads

$$a_\mu^{\text{bos},2L,\text{MSSM}} = \frac{5}{3} \frac{G_\mu m_\mu^2}{8\pi^2 \sqrt{2}} \frac{\alpha}{\pi} \left(c_L^{\text{bos},2L,\text{MSSM}} \log \frac{m_\mu^2}{M_W^2} + c_0^{\text{bos},2L,\text{MSSM}} \right) \quad (25)$$

where the coefficient of the logarithm is given by

$$c_L^{\text{bos},2L,\text{MSSM}} = \frac{1}{30} [98 + 9c_L^h + 23(1 - 4s_w^2)^2], \quad (26)$$

$$c_L^h = \frac{c_{2\beta} M_Z^2}{c_\beta} \left[\frac{c_\alpha c_{\alpha+\beta}}{m_H^2} + \frac{s_\alpha s_{\alpha+\beta}}{m_h^2} \right]. \quad (27)$$

Here β is defined by the ratio of the two Higgs-vacuum expectation values, $\tan \beta = v_2/v_1$; $m_{h,H}$ and α are the masses and the mixing angle in the \mathcal{CP} -even Higgs sector, and $c_\alpha \equiv \cos \alpha$, etc. As we will discuss below, $c_L^h = 1$, and thus the logarithms in the SM and the MSSM are identical.

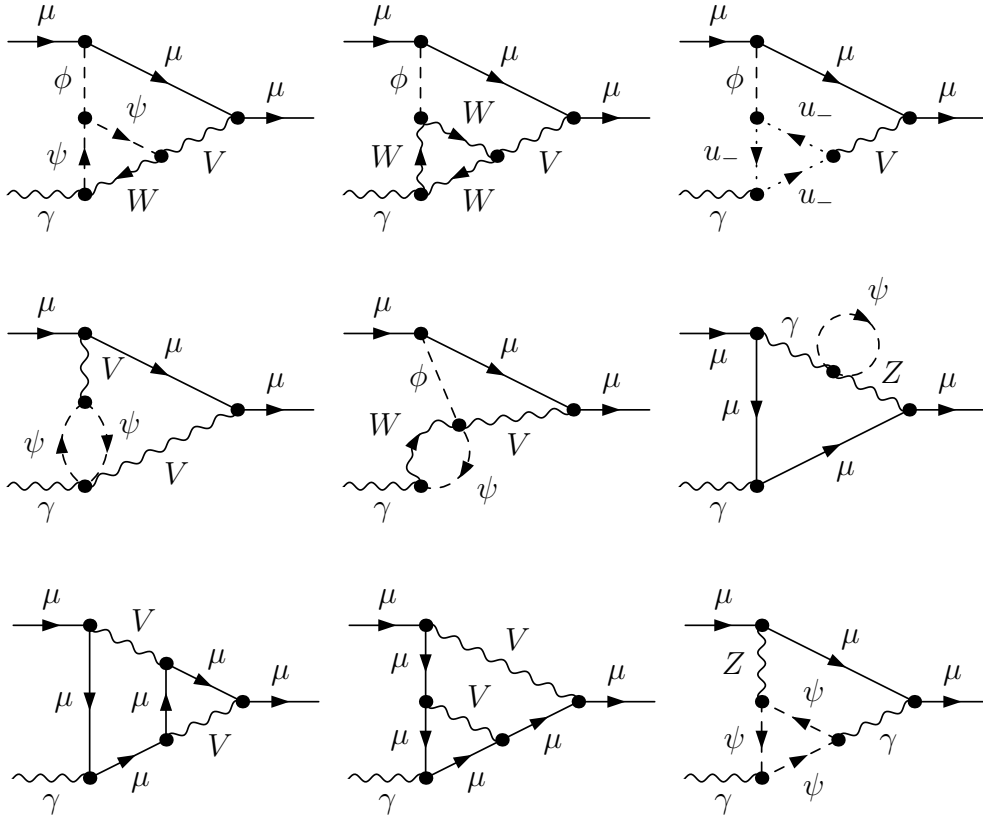


Figure 3: Some two-Higgs-doublet model diagrams for a_μ with (depending on the diagram) $\phi = h, H, A, G$; $\psi = G^\pm, H^\pm$; $V = \gamma, Z$.

Let us first comment on the non-logarithmic contribution in (25). The non-logarithmic coefficient $c_0^{\text{bos},2\text{L},\text{MSSM}}$ is a complicated function of the full MSSM Higgs sector, which is determined by two parameters, $\tan\beta$ and the pseudo-scalar Higgs-boson mass M_A . However, in Fig. 4 it is demonstrated that the full results for $a_\mu^{\text{bos},2\text{L},\text{MSSM}}$ can be quite well approximated by the corresponding SM quantity if $M_{H^{\text{SM}}}$ is set equal to the light \mathcal{CP} -even Higgs-boson mass of the MSSM, $M_{H^{\text{SM}}} = m_h$, except in parameter scenarios with extremely light \mathcal{CP} -odd Higgs-boson mass. For $M_A \gtrsim 100$ GeV the difference stays below 0.3×10^{-10} . The difference between the MSSM and the SM comes solely from the different coefficients $c_0^{\text{bos},2\text{L},\text{MSSM}}$ and $c_0^{\text{bos},2\text{L}}$.

As in the SM, the logarithmic piece in (25) is an excellent approximation of the full bosonic result. At first sight, the coefficient (26) seems different from the corresponding SM one, owing to the appearance of Higgs-mass dependent terms. However, the MSSM Higgs-masses satisfy the relation

$$\frac{c_{2\beta} M_Z^2}{c_\beta} \left[\frac{c_\alpha c_{\alpha+\beta}}{m_H^2} + \frac{s_\alpha s_{\alpha+\beta}}{m_h^2} \right] = 1 \quad (28)$$

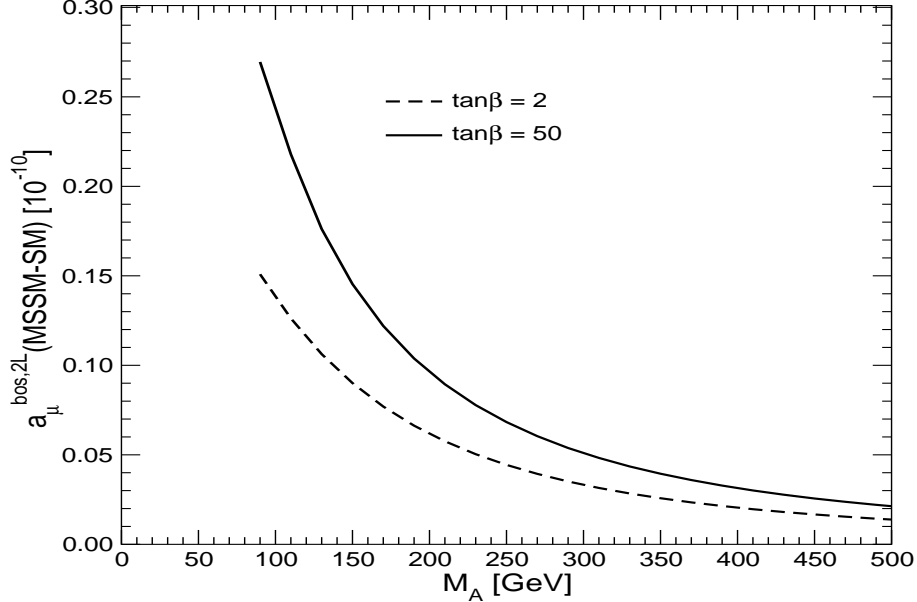


Figure 4: The difference of $a_\mu^{\text{bos},2L}$ in the MSSM and the SM is shown as a function of M_A . The SM Higgs-boson mass has been set equal to the light \mathcal{CP} -even MSSM Higgs mass. $\tan\beta$ has been set to $\tan\beta = 2, 50$. The differences between the MSSM and the SM come solely from the different coefficients $c_0^{\text{bos},2L,\text{MSSM}}$ and $c_0^{\text{bos},2L}$.

at tree-level. Hence, the coefficient $c_L^h = 1$ in (26), and the logarithmic pieces of the MSSM and SM bosonic two-loop corrections are identical as mentioned above. This finding can be explained in several different ways. One way is to apply the analysis of the $\log \frac{m_\mu^2}{M_W^2}$ -terms performed in Ref. [14] to the bosonic contributions. This shows that they must be identical in the SM and MSSM since the corresponding bosonic one-loop diagrams are identical. The latter statement is true since the additional MSSM Higgs bosons do not appear at the one-loop level, in particular since there is no $\gamma W^\pm H^\mp$ -coupling.⁴

Alternatively, one can directly investigate the first Feynman diagram in Fig. 3 (with $\phi = h, H$ and $\psi = G^\pm$) in order to understand how the logarithms in the SM and MSSM emerge. The diagrams with photon and physical Higgs exchange and an inner $G^\pm - W^\pm$ loop are responsible for the Higgs-mass dependence in the coefficients of $\log \frac{m_\mu^2}{M_W^2}$. In the corresponding SM diagram (with $\phi = H^{\text{SM}}$) the $G^+ G^- H^{\text{SM}}$ -coupling is proportional to $M_{H^{\text{SM}}}^2/M_W$, and the dependence on $M_{H^{\text{SM}}}$ exactly cancels with the suppression coming from the Higgs propagator. In the MSSM the couplings of G^\pm to physical Higgs bosons are given by gauge couplings, hence leading to the structure of

⁴More precisely, the additional MSSM Higgs bosons as well as the SM Higgs boson do appear in one-loop diagrams, but their contributions are suppressed by two additional muon Yukawa couplings and hence negligible.

c_L^h shown above in eq. (27) and to the seeming $m_{h,H}$ -dependence of the logarithm.

However, as the appearance of Goldstone bosons signals, such Feynman diagrams are not gauge independent by themselves. For example, in the unitary gauge there are no Goldstone bosons and such diagrams do not exist. Similarly, in the background field gauge [41] or in the nonlinear gauge used in Ref. [12] there is no $\gamma W^\pm G^\mp$ -vertex, and again the diagrams in Fig. 3 do not exist. In all these gauges there are no diagrams with virtual photon and physical Higgs, hence it is manifest that the logarithms in the SM and MSSM are identical.

In the Feynman gauge, which we we have chosen, this fact is not immediately obvious but follows from relation (28), which in turn is a consequence of global gauge invariance. In fact, one can easily derive that the Higgs mass matrix $\Gamma_{\phi_i\phi_j}$ (corresponding to the denominators in (28)), where $\phi_{i,j}$ are the \mathcal{CP} -even interaction Higgs eigenstates, is related to the couplings $\Gamma_{\phi_i G^+ G^-}$ (corresponding to the numerators in (28)).⁵

This discussion has a practical implication concerning the treatment of higher-order contributions to the Higgs-boson masses. In other sectors like the sfermion-loop or chargino/neutralino-loop sector, leading three-loop effects can be taken into account by using the loop-corrected values for the Higgs-boson masses $M_{h,H}$ in the propagators. In the present sector, however, using loop-corrected Higgs-boson masses would spoil the validity of (28), which is required by gauge invariance. Three-loop effects in the Higgs propagators would be taken into account but three-loop effects in the couplings $\Gamma_{\phi_i G^+ G^-}$ would be neglected, resulting in fake large effects. Therefore, tree-level Higgs-boson masses have to be used in the propagators for the bosonic two-loop contributions (as has been done in Fig. 4).

The shift induced by replacing the tree-level Higgs-boson masses by loop corrected masses in the two-loop contributions gives an indication of the possible size of bosonic three-loop corrections. A shift of $\mathcal{O}(50 \text{ GeV})$ in m_h induces a variation in a_μ of up to about 0.2×10^{-10} as shown in Fig. 2, which can be regarded as a three-loop uncertainty.

5 Chargino/neutralino loop contributions

The 2-loop contributions to a_μ containing a closed chargino/neutralino loop constitute a separately UV-finite and gauge-independent class. The corresponding diagrams are shown in Fig. 5. In this section we discuss the numerical impact and the parameter dependence of this class.

The chargino/neutralino two-loop contributions, $a_\mu^{\chi,2L}$, depend on the mass parameters for the charginos and neutralinos μ , $M_{1,2}$, the \mathcal{CP} -odd Higgs mass M_A , and $\tan \beta$.

⁵In Ref. [42], eqs. (27,28), a similar relation between the Higgs mass matrix $\Gamma_{\phi_i\phi_j}$ and the gauge dependence of tadpole diagrams has been derived. Gauge dependent tadpole diagrams are in particular the ones with G^\pm loops, thus involving the coupling $\Gamma_{\phi_i G^+ G^-}$, so that this constitutes again a gauge relation between $\Gamma_{\phi_i\phi_j}$ and $\Gamma_{\phi_i G^+ G^-}$.

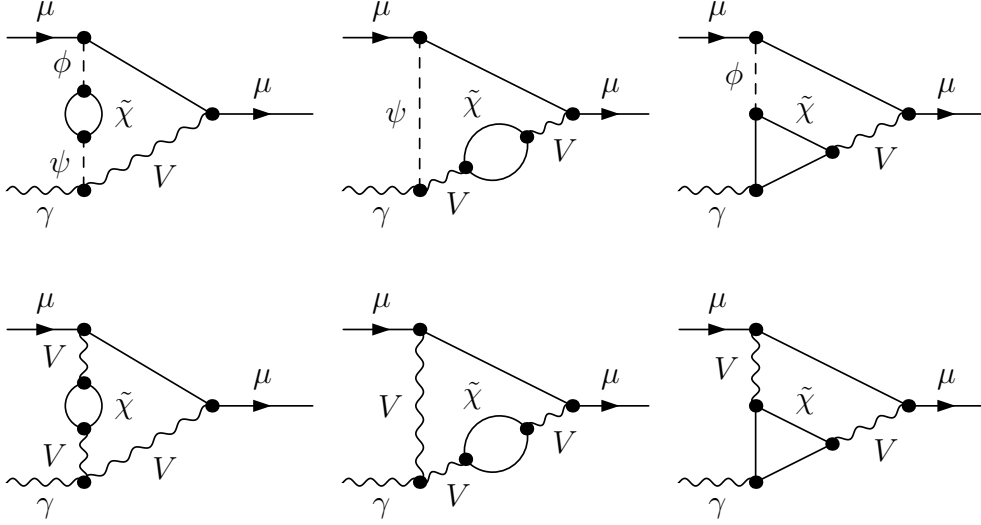


Figure 5: Generic two-loop diagrams to a_μ with a closed chargino/neutralino loop. ϕ , ψ denote the scalar particles h , H , A^0 , H^\pm and $G^{0,\pm}$; V denotes the vector bosons γ , Z , W^\pm ; $\tilde{\chi}$ stands for the chargino/neutralino mass eigenstates $\tilde{\chi}_{1,2}^\pm$, $\tilde{\chi}_{1,2,3,4}^0$.

Since we use the loop-corrected values for the \mathcal{CP} -even Higgs masses $M_{h,H}$ [20, 21, 27] in the propagators for this class of diagrams, formally an effect of 3-loop order, $a_\mu^{\chi,2L}$ also has a slight dependence on other MSSM parameters through $M_{h,H}$ (we denote the loop-corrected masses as $M_{h,H}$ and the tree-level masses as $m_{h,H}$; see also the discussion in Sect. 4). It is interesting to note that, contrary to Ref. [24], no tree-level relations in the Higgs sector were needed in order to find a UV-finite result. This is due to the fact that each two-loop diagram contributing to $(g-2)_\mu$ together with its corresponding subloop renormalization is finite.

It turns out that the parameter dependence of $a_\mu^{\chi,2L}$ is quite straightforward. If all supersymmetric mass scales are set equal,⁶ $\mu = M_2 = M_A \equiv M_{\text{SUSY}}$, the approximate leading behaviour of $a_\mu^{\chi,2L}$ is simply given by $\tan\beta/M_{\text{SUSY}}^2$, and we find the approximate relation

$$a_\mu^{\chi,2L} \approx 11 \times 10^{-10} \left(\frac{\tan\beta}{50} \right) \left(\frac{100 \text{ GeV}}{M_{\text{SUSY}}} \right)^2 \text{sign}(\mu). \quad (29)$$

As shown in Fig. 6, the approximation is very good except for very small M_{SUSY} and small $\tan\beta$, where the leading term is suppressed by the small μ , and subleading terms begin to dominate.

The chargino/neutralino sector does not only contribute to $a_\mu^{\chi,2L}$ but already to $a_\mu^{\text{SUSY},1L}$, so it is interesting to compare the one- and two-loop contributions. For

⁶For simplicity we assume throughout this paper that $M_{1,2}$ are related by the GUT relation $M_1 = 5/3 s_w^2/c_w^2 M_2$.

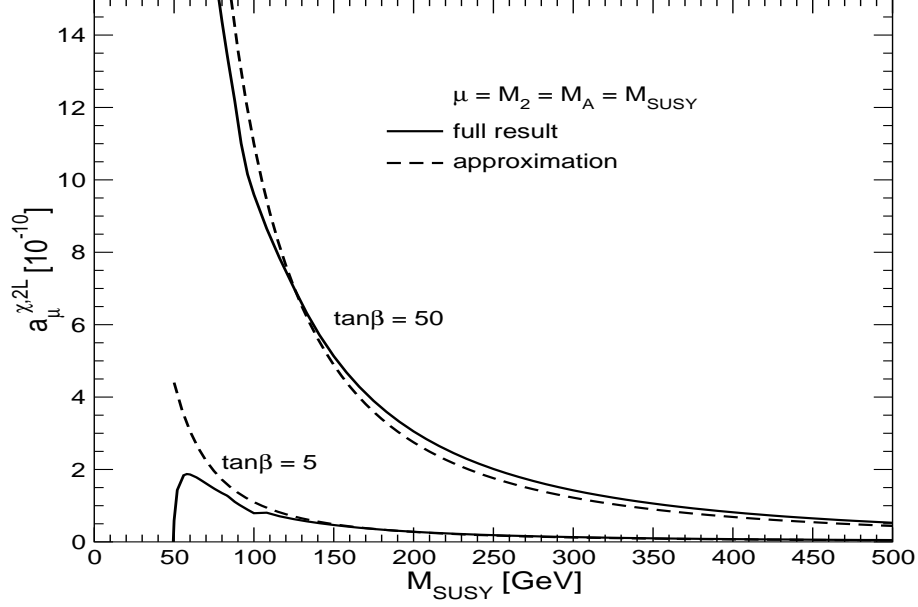


Figure 6: Comparison of the full result for $a_\mu^{\chi,2L}$ with the approximation (29) for $\mu = M_2 = M_A \equiv M_{\text{SUSY}}$. The full lines show the complete result, while the dashed lines indicate the approximation. For the upper curves $\tan\beta = 50$ has been used, for the lower ones $\tan\beta = 5$.

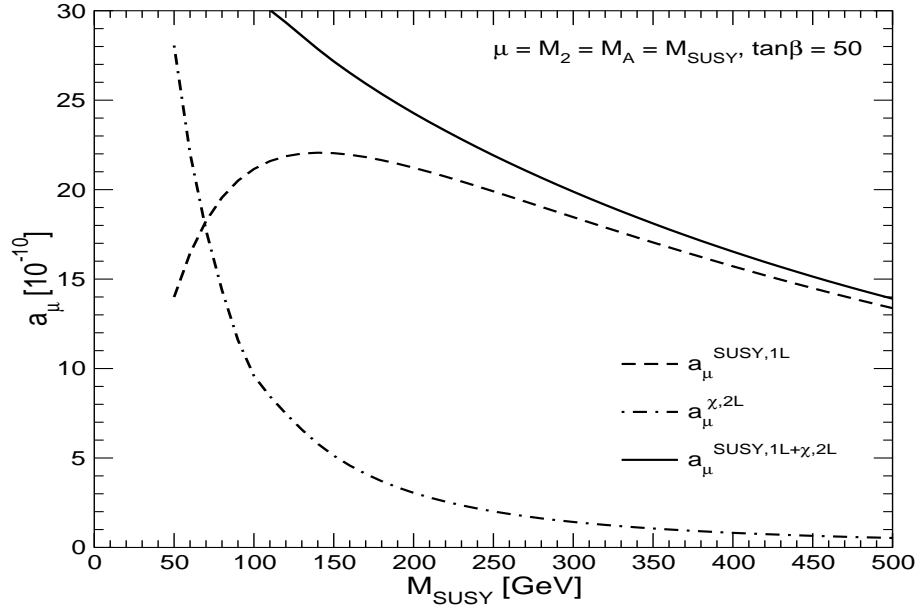


Figure 7: Comparison of the supersymmetric one-loop result $a_\mu^{\text{SUSY},1L}$ (dashed) with the two-loop chargino/neutralino contributions $a_\mu^{\chi,2L}$ (dash-dotted) and the sum (full line). The parameters are $\mu = M_2 = M_A \equiv M_{\text{SUSY}}$, $\tan\beta = 50$, and the sfermion mass parameters are set to 1TeV.

the case that all masses, including the smuon and sneutrino masses, are set equal to M_{SUSY} , the one-loop and two-loop contributions can be trivially compared using eqs. (5), (29), showing that the two-loop contribution shifts the one-loop result by about 2%.

However, the chargino/neutralino sector might very well be significantly lighter than the slepton sector of the second generation, in particular in the light of FCNC and \mathcal{CP} -violating constraints, which are more easily satisfied for heavy 1st and 2nd generation sfermions. In Fig. 7 the chargino/neutralino two-loop contributions are therefore compared with the supersymmetric one-loop contribution $a_\mu^{\text{SUSY,1L}}$ at fixed high smuon and sneutrino masses $M_{\tilde{l}} = 1$ TeV. The other masses are again set equal, $\mu = M_2 = M_A \equiv M_{\text{SUSY}}$. Furthermore, we use a large $\tan\beta$ value, $\tan\beta = 50$, which enhances the SUSY contributions to a_μ .

We find that for $M_{\text{SUSY}} \lesssim 400$ GeV the two-loop contributions become more and more important. For $M_{\text{SUSY}} \approx 100$ GeV they even amount to 50% of the one-loop contributions, which are suppressed by the large smuon and sneutrino masses.

It is noteworthy that in the numerical analysis of the sfermion loop contributions in Ref. [15] it was crucial to take into account the experimental constraints on the light Higgs-boson mass M_h [18–21], electroweak precision observables [22–24] and the b -decays $B \rightarrow X_s \gamma$ and $B_s \rightarrow \mu^+ \mu^-$ [25, 26]. In the case of chargino/neutralino loop contributions, however, these experimental constraints have only little impact on the possible choices of μ , M_2 and M_A since the relevant observables depend strongly on the 3rd generation sfermion mass parameters.

From Figs. 6, 7 one can read off that the chargino/neutralino two-loop contributions can amount to about $\pm 10 \times 10^{-10}$ if μ , M_2 , and M_A are around 100 GeV. This parameter region is rather constrained but not entirely excluded by the experimental bounds from direct searches for charginos and neutralinos, from Higgs searches and from b -physics.

The dependence of $a_\mu^{\text{SUSY,1L}} + a_\mu^{\chi,2\text{L}}$ and $a_\mu^{\text{SUSY,1L}}$ on μ and M_2 is shown in the contour plots of Fig. 8. We fix $M_A = 200$ GeV and vary $\tan\beta$ and the common smuon and sneutrino mass $M_{\tilde{l}}$, which has an impact only on the one-loop contribution. We have checked that these parameter choices are allowed essentially in the entire μ - M_2 -plane by the current experimental constraints mentioned above, provided the \tilde{t} and \tilde{b} mass parameters are of $\mathcal{O}(1$ TeV). The contours drawn in Fig. 8 correspond to the 1σ , 2σ , ... regions around the value $a_\mu^{\text{exp}} - a_\mu^{\text{theo,SM}} = (24.5 \pm 9.0) \times 10^{-10}$, based on Refs. [3, 7]. We find that for the investigated parameter space the SUSY prediction for a_μ lies mostly in the $0 - 2\sigma$ region if μ is positive. However, the new two-loop corrections shift the 1σ and 2σ contours considerably. This effect is more pronounced for smaller $\tan\beta$ and larger $M_{\tilde{l}}$.

The M_A -dependence of the pure two-loop contributions $a_\mu^{\chi,2\text{L}}$ is shown in Fig. 9 for μ , $M_2 = 150, 500$ GeV. For the smaller values of μ and M_2 , $a_\mu^{\chi,2\text{L}}$ behaves approximately as $1/M_A$; for the larger values of μ and M_2 the M_A -dependence is less

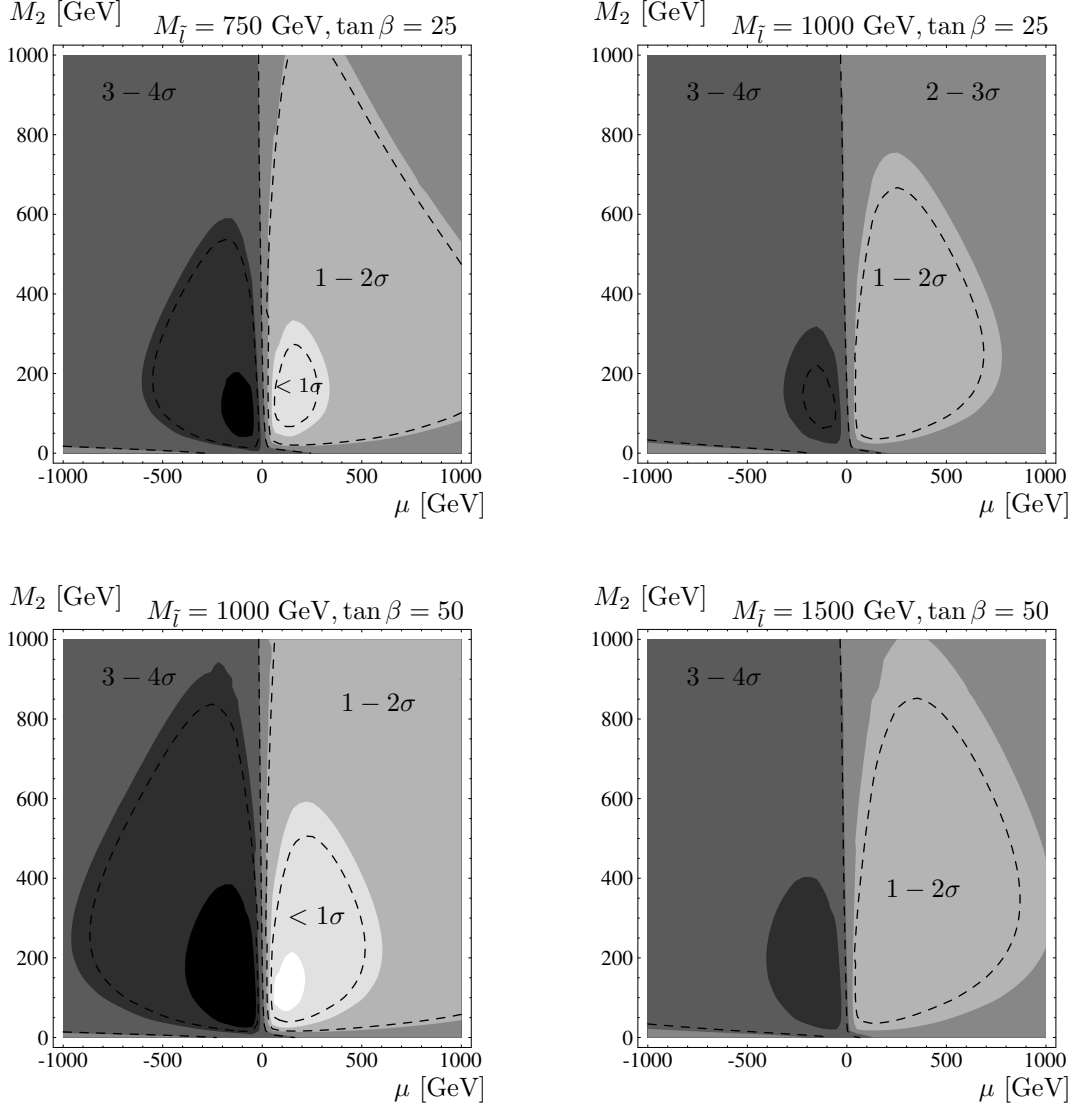


Figure 8: Contours of $a_\mu^{\text{SUSY,1L}} + a_\mu^{\chi,2\text{L}}$ (solid border) and $a_\mu^{\text{SUSY,1L}}$ alone (dashed line) in the μ - M_2 -plane for $M_A = 200$ GeV. The slepton mass scale (which enters only the one-loop prediction) and $\tan\beta$ are indicated for each plot. The contours are at $(24.5, 15.5, 6.5, -2.5, -11.5, -20.5) \times 10^{-10}$ corresponding to the central value of $a_\mu^{\text{exp}} - a_\mu^{\text{theo,SM}} = (24.5 \pm 9.0) \times 10^{-10}$ and intervals of 1-5 σ .

pronounced.

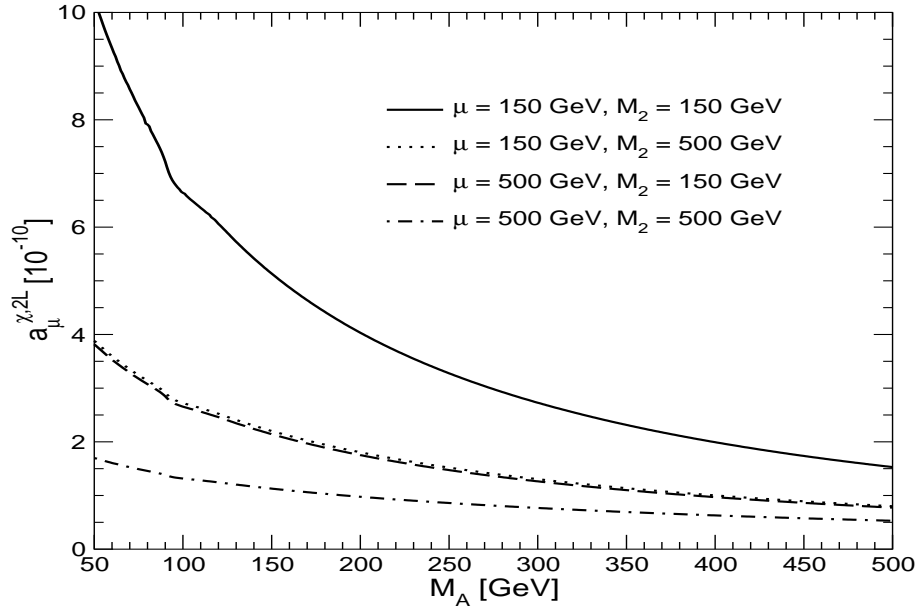


Figure 9: Dependence of $a_\mu^{\chi,2L}$ on the \mathcal{CP} -odd Higgs mass M_A for $\tan\beta = 50$ and $\mu = M_2 = 150, 500$ GeV.

6 Conclusions

We have calculated two kinds of two-loop contributions to $(g-2)_\mu$: the purely bosonic two-loop corrections (diagrams involving μ , ν_μ , gauge and Higgs bosons) in the SM and the MSSM, and the two-loop corrections involving a neutralino/chargino subloop in the MSSM.

In the SM our calculation provides an independent check and a slight extension of Refs. [12,13], which was up to now the only calculation of the bosonic two-loop corrections, using the approximation $M_{HSM} \gg M_W$. We find good agreement with Refs. [12,13]. The variation with M_{HSM} is at the level of 0.3×10^{-10} for $100 \text{ GeV} \lesssim M_{HSM} \lesssim 500 \text{ GeV}$. The final result can be well approximated by the M_{HSM} -independent logarithmic piece, eq. (23), $a_\mu^{\text{bos},2L} = (-2.2 \pm 0.2) \times 10^{-10}$, where the central value corresponds to $M_{HSM} \approx 200 \text{ GeV}$.

In the MSSM our calculation completes the program begun in Ref. [15] to calculate all MSSM two-loop corrections to two-Higgs-doublet model one-loop diagrams. This class of corrections has a potentially larger impact on the MSSM prediction of $(g-2)_\mu$ than the higher-order corrections to purely SUSY one-loop diagrams, since it is not suppressed in case the smuon and sneutrino masses are large. In addition to the SM fermion and scalar fermion loop corrections derived in Ref. [15], we have calculated

here the diagrams with a neutralino/chargino loop as well as the purely bosonic two-loop diagrams in the MSSM (i.e. diagrams involving no SUSY particles).

For the purely bosonic two-loop corrections in the MSSM we find only a small deviation from the SM result. The logarithmic piece is identical, while the non-logarithmic piece causes only a difference in a_μ below the level of 0.3×10^{-10} compared to the SM result with a light Higgs. The result for the purely bosonic two-loop corrections in the MSSM lies in the range $-1.5 \times 10^{-10} \lesssim a_\mu^{\text{bos},2\text{L},\text{MSSM}} \lesssim -2.0 \times 10^{-10}$, depending on the values of M_A and $\tan\beta$.

A sizable shift, on the other hand, arises from the two-loop contributions where a neutralino/chargino loop is inserted into a two-Higgs-doublet model one-loop diagram. Depending on the values of μ , M_2 , M_A , and $\tan\beta$, the result can amount up to $\pm 10 \times 10^{-10}$. For example, if all masses are set equal to a common scale M_{SUSY} we find the approximate relation

$$a_\mu^{\chi,2\text{L}} \approx 11 \times 10^{-10} \left(\frac{\tan\beta}{50} \right) \left(\frac{100 \text{ GeV}}{M_{\text{SUSY}}} \right)^2 \text{sign}(\mu) . \quad (30)$$

Thus, the regions in the MSSM parameter space which satisfy the requirement that a_μ agrees with the experimental value at the 2σ level can be shifted significantly as a consequence of the new two-loop corrections.

The analytical results presented here will be implemented into the Fortran code *FeynHiggs* (see: www.feynhiggs.de). Based on the new results presented in this paper, the last missing piece of the MSSM two-loop contributions to $(g-2)_\mu$ are the two-loop corrections to the SUSY one-loop diagrams. Their inclusion, which will be desirable in order to further reduce the theoretical uncertainty, will constitute the first complete two-loop result within the MSSM.

Acknowledgements

S.H. thanks the Institute for Particle Physics Phenomenology (IPPP), University of Durham, for hospitality during the early stages of this work. D.S. thanks the CERN Theory division for hospitality when finalizing this work. G.W. thanks B. Krause for interesting discussions in the early stages of this work.

References

- [1] [The Muon $g-2$ Collaboration], *Phys. Rev. Lett.* **92** (2004) 161802, hep-ex/0401008.
- [2] M. Davier, S. Eidelman, A. Höcker and Z. Zhang, *Eur. Phys. J. C* **31** (2003) 503, hep-ph/0308213.

- [3] K. Hagiwara, A. Martin, D. Nomura and T. Teubner, *Phys. Rev. D* **69** (2004) 093003, hep-ph/0312250.
- [4] S. Ghozzi and F. Jegerlehner, *Phys. Lett. B* **583** (2004) 222, hep-ph/0310181.
- [5] J. de Troconiz and F. Yndurain, hep-ph/0402285.
- [6] M. Knecht and A. Nyffeler, *Phys. Rev. D* **65** (2002) 073034, hep-ph/0111058;
M. Knecht, A. Nyffeler, M. Perrottet and E. De Rafael, *Phys. Rev. Lett.* **88** (2002) 071802, hep-ph/0111059;
I. Blokland, A. Czarnecki and K. Melnikov, *Phys. Rev. Lett.* **88** (2002) 071803, hep-ph/0112117;
M. Ramsey-Musolf and M. Wise, *Phys. Rev. Lett.* **89** (2002) 041601, hep-ph/0201297;
J. Kühn, A. Onishchenko, A. Pivovarov and O. Veretin, *Phys. Rev. D* **68** (2003) 033018, hep-ph/0301151.
- [7] K. Melnikov and A. Vainshtein, hep-ph/0312226.
- [8] T. Kinoshita and M. Nio, hep-ph/0402206.
- [9] T. Moroi, *Phys. Rev. D* **53** (1996) 6565 [Erratum-ibid. *D* **56** (1997) 4424], hep-ph/9512396.
- [10] J. Ellis, D. Nanopoulos and K. Olive, *Phys. Lett. B* **508** (2001) 65, hep-ph/0102331;
R. Arnowitt, B. Dutta, B. Hu and Y. Santoso, *Phys. Lett. B* **505** (2001) 177, hep-ph/0102344;
J. Ellis, S. Heinemeyer, K. Olive and G. Weiglein, *Phys. Lett. B* **515** (2001) 348, hep-ph/0105061; *JHEP* **0301** (2003) 006, hep-ph/0211206;
A. Djouadi, M. Drees and J. Kneur, *JHEP* **0108** (2001) 055, hep-ph/0107316.
- [11] L. Everett, G. Kane, S. Rigolin and L. Wang, *Phys. Rev. Lett.* **86** (2001) 3484, hep-ph/0102145;
J. Feng and K. Matchev, *Phys. Rev. Lett.* **86** (2001) 3480, hep-ph/0102146;
U. Chattopadhyay and P. Nath, *Phys. Rev. Lett.* **86** (2001) 5854, hep-ph/0102157;
S. Komine, T. Moroi and M. Yamaguchi, *Phys. Lett. B* **506** (2001) 93, hep-ph/0102204;
S. Martin and J. Wells, *Phys. Rev. D* **64** (2001) 035003, hep-ph/0103067;
H. Baer, C. Balazs, J. Ferrandis and X. Tata, *Phys. Rev. D* **64** (2001) 035004, hep-ph/0103280;
S. Martin and J. Wells, *Phys. Rev. D* **67** (2003) 015002, hep-ph/0209309.
- [12] A. Czarnecki, B. Krause and W. Marciano, *Phys. Rev. Lett.* **76** (1996) 3267, hep-ph/9512369; *Phys. Rev. D* **52** (1995) 2619, hep-ph/9506256.

- [13] B. Krause, PhD thesis, Universität Karlsruhe, 1997, Shaker Verlag, ISBN 3-8265-2780-1.
- [14] G. Degrassi and G. Giudice, *Phys. Rev. D* **58** (1998) 053007, hep-ph/9803384.
- [15] S. Heinemeyer, D. Stöckinger and G. Weiglein, to appear in *Nucl. Phys. B*, hep-ph/0312264.
- [16] C. Chen and C. Geng, *Phys. Lett. B* **511** (2001) 77, hep-ph/0104151.
- [17] A. Arhrib and S. Baek, *Phys. Rev. D* **65** (2002) 075002, hep-ph/0104225.
- [18] [LEP Higgs working group], hep-ex/0107030; LHWG Note 2001-4, see: lephiggs.web.cern.ch/LEPHIGGS/papers/ .
- [19] [LEP Higgs working group], *Phys. Lett. B* **565** (2003) 61, hep-ex/0306033.
- [20] S. Heinemeyer, W. Hollik and G. Weiglein, *Eur. Phys. J. C* **9** (1999) 343, hep-ph/9812472.
- [21] G. Degrassi, S. Heinemeyer, W. Hollik, P. Slavich and G. Weiglein, *Eur. Phys. J. C* **28** (2003) 133, hep-ph/0212020.
- [22] M. Drees and K. Hagiwara, *Phys. Rev. D* **42** (1990) 1709.
- [23] A. Djouadi, P. Gambino, S. Heinemeyer, W. Hollik, C. Jünger and G. Weiglein, *Phys. Rev. Lett.* **78** (1997) 3626, hep-ph/9612363; *Phys. Rev. D* **57** (1998) 4179, hep-ph/9710438.
- [24] S. Heinemeyer and G. Weiglein, *JHEP* **0210** (2002) 072, hep-ph/0209305; hep-ph/0301062.
- [25] F. Azfar, *eConf C030626* (2003) FRAT05, hep-ex/0309005;
M. Nakao,[BELLE Collaboration], *eConf C0304052* (2003) WG208, hep-ex/0307031;
K. Babu and C. Kolda, *Phys. Rev. Lett.* **84** (2000) 228, hep-ph/9909476;
S. Choudhury and N. Gaur, *Phys. Lett. B* **451** (1999) 86, hep-ph/9810307;
C. Bobeth, T. Ewerth, F. Kruger and J. Urban, *Phys. Rev. D* **64** (2001) 074014, hep-ph/0104284;
A. Dedes, H. Dreiner and U. Nierste, *Phys. Rev. Lett.* **87** (2001) 251804, hep-ph/0108037;
G. Isidori and A. Retico, *JHEP* **0111** (2001) 001, hep-ph/0110121;
A. Dedes and A. Pilaftsis, *Phys. Rev. D* **67** (2003) 015012, hep-ph/0209306;
A. Buras, P. Chankowski, J. Rosiek and L. Slawianowska, *Nucl. Phys. B* **659** (2003) 3, hep-ph/0210145;
A. Dedes, *Mod. Phys. Lett. A* **18** (2003) 2627, hep-ph/0309233.

- [26] P. Cho, M. Misiak and D. Wyler, *Phys. Rev. D* **54**, 3329 (1996), hep-ph/9601360;
A. Kagan and M. Neubert, *Eur. Phys. J. C* **7** (1999) 5, hep-ph/9805303;
K. Chetyrkin, M. Misiak and M. Münz, *Phys. Lett. B* **400**, (1997) 206, [Erratum-
ibid. **B 425** (1998) 414] hep-ph/9612313;
P. Gambino and M. Misiak, *Nucl. Phys. B* **611** (2001) 338, hep-ph/0104034;
A. Ali, E. Lunghi, C. Greub and G. Hiller, *Phys. Rev. D* **66** (2002) 034002,
hep-ph/0112300;
R. Barate et al. [ALEPH Collaboration], *Phys. Lett. B* **429** (1998) 169;
S. Chen et al. [CLEO Collaboration], *Phys. Rev. Lett.* **87** (2001) 251807,
hep-ex/0108032;
K. Abe et al. [Belle Collaboration], *Phys. Lett. B* **511** (2001) 151,
hep-ex/0103042;
B. Aubert et al. [BABAR Collaboration], hep-ex/0207074; hep-ex/0207076.
- [27] S. Heinemeyer, W. Hollik and G. Weiglein, *Comp. Phys. Comm.* **124** (2000) 76,
hep-ph/9812320; hep-ph/0002213;
M. Frank, S. Heinemeyer, W. Hollik and G. Weiglein, hep-ph/0202166.
The codes are accessible via www.feynhiggs.de .
- [28] W. Siegel, *Phys. Lett.* **84** (1979) 193.
- [29] W. Beenakker, R. Höpker and P. Zerwas, *Phys. Lett. B* **378** (1996) 159,
hep-ph/9602378;
W. Hollik, E. Kraus and D. Stöckinger, *Eur. Phys. J. C* **11** (1999) 365,
hep-ph/9907393;
W. Hollik and D. Stöckinger, *Eur. Phys. J. C* **20** (2001) 105, hep-ph/0103009;
W. Hollik, E. Kraus, M. Roth, C. Rupp, K. Sibold and D. Stöckinger, *Nucl.*
Phys. B **639** (2002) 3, hep-ph/0204350;
I. Fischer, W. Hollik, M. Roth and D. Stöckinger, *Phys. Rev. D* **69** (2004) 015004,
hep-ph/0310191.
- [30] A. Freitas, W. Hollik, W. Walter and G. Weiglein, *Phys. Lett. B* **495** (2000) 338
[Erratum-ibid. **B 570** (2003) 260], hep-ph/0007091; *Nucl. Phys. B* **632** (2002)
189 [Erratum-ibid. **B 666** (2003) 305], hep-ph/0202131.
- [31] G. 't Hooft and M. Veltman, *Nucl. Phys. B* **44** (1972) 189;
P. Breitenlohner and D. Maison, *Commun. Math. Phys.* **52** (1977) 11.
- [32] J. Küblbeck, M. Böhm, and A. Denner, *Comput. Phys. Commun.* **60** (1990) 165;
T. Hahn, *Comput. Phys. Commun.* **140** (2001) 418, hep-ph/0012260.
- [33] T. Hahn and C. Schappacher, *Comput. Phys. Commun.* **143** (2002) 54,
hep-ph/0105349.
- [34] G. Weiglein, R. Scharf and M. Böhm, *Nucl. Phys. B* **416** (1994) 606,
hep-ph/9310358;

- G. Weiglein, R. Mertig, R. Scharf and M. Böhm, in *New Computing Techniques in Physics Research 2*, ed. D. Perret-Gallix (World Scientific, Singapore, 1992), p. 617.
- [35] V. Smirnov, *Applied Asymptotic Expansions in Momenta and Masses*, Springer Verlag, Berlin (2002).
- [36] K Chetyrkin and F. Tkachov, *Nucl. Phys. B* **192** (1981) 159.
- [37] A. Davydychev und J. Tausk, *Nucl. Phys. B* **397** (1993) 123;
F. Berends und J. Tausk, *Nucl. Phys. B* **421** (1994) 456.
- [38] G. Passarino and M. Veltman, *Nucl. Phys. B* **160** (1979) 151.
- [39] J. Fleischer and M. Kalmykov, *Comput. Phys. Commun.* **128** (2000) 531, hep-ph/9907431.
- [40] B. Lautrup and E. De Rafael, *Phys. Rev.***174**, 1835 (1968);
M. Samuel and G. w. Li, *Phys. Rev. D* **44** (1991) 3935, [Erratum-ibid. **D 48** (1993) 1879].
- [41] A. Denner, G. Weiglein and S. Dittmaier, *Nucl. Phys. B* **440** (1995) 95, hep-ph/9410338.
- [42] A. Freitas and D. Stöckinger, *Phys. Rev. D* **66** (2002) 095014, hep-ph/0205281.